2D-GDS measurements in the southern Gawler Craton, SA Australia and derived tectonics

Stephan Thiel[1] **and Graham Heinson**
Continental Evolution Research Group
School of Earth and Environmental Sciences
University of Adelaide, Adelaide SA 5005, Australia
Tel: 08-8303-5377 Fax: 08-8303-4347
E-mail: Thiel.Stephan@gmx.de
E-mail: Graham.Heinson@adelaide.edu.au

Antony White
School of Physics, Chemistry and Earth Sciences
Flinders University of South Australia
GPO Box 2100, Adelaide SA 5001, Australia
Tel: 08-8201-2020 Fax: 08-8201-2676
E-mail: Antony.White@flinders.edu.au

Abstract

Long-period natural-source electromagnetic (EM) data have been recorded using portable three-component magnetometers at forty sites in 1998 and 2002 across the southern Eyre Peninsula, South Australia. Two profiles trending east-west were inverted for two-dimensional (2D) electrical resistivity models delineating the Eyre Peninsula Anomaly (EPA) and the Kalinjala Shear Zone, and help constrain the tectonic evolution of the southern Gawler Craton during the period 2.00-1.70 Ga. The main features from the models are (a) the Kalinjala Shear Zone dips slightly to the west suggesting, that it is a growth fault; (b) the EPA is a shallow highly electrically conductive synclinal structure; (c) a further conductive zone is coincident with known graphite deposits. The Sequence of extension and compression events led to deposition of carbonaceous sediments in a shallow sea and further metamorphosis into graphite including migration to fold hinges and further concentration.

1 Introduction

In the last thirty years long-period EM surveys have unveiled a number of major crustal anomalies throughout Australia. White & Milligan (1984) revealed the existence of a low resistivity zone within the late Archaean - early Proterozoic Gawler Craton in southern Eyre Peninsula in South Australia. The Eyre Peninsula Anomaly (EPA) has since been focus of a number of studies (Milligan *et al.*, 1989; Popkov *et al.*, 2000). The EPA is embedded in the southern Gawler Craton, parallel to magnetic lineations caused by banded iron formations (Figure 1). To the west of the EPA there are some exposures of Archaean

[1] now at TU BA Freiberg, Germany

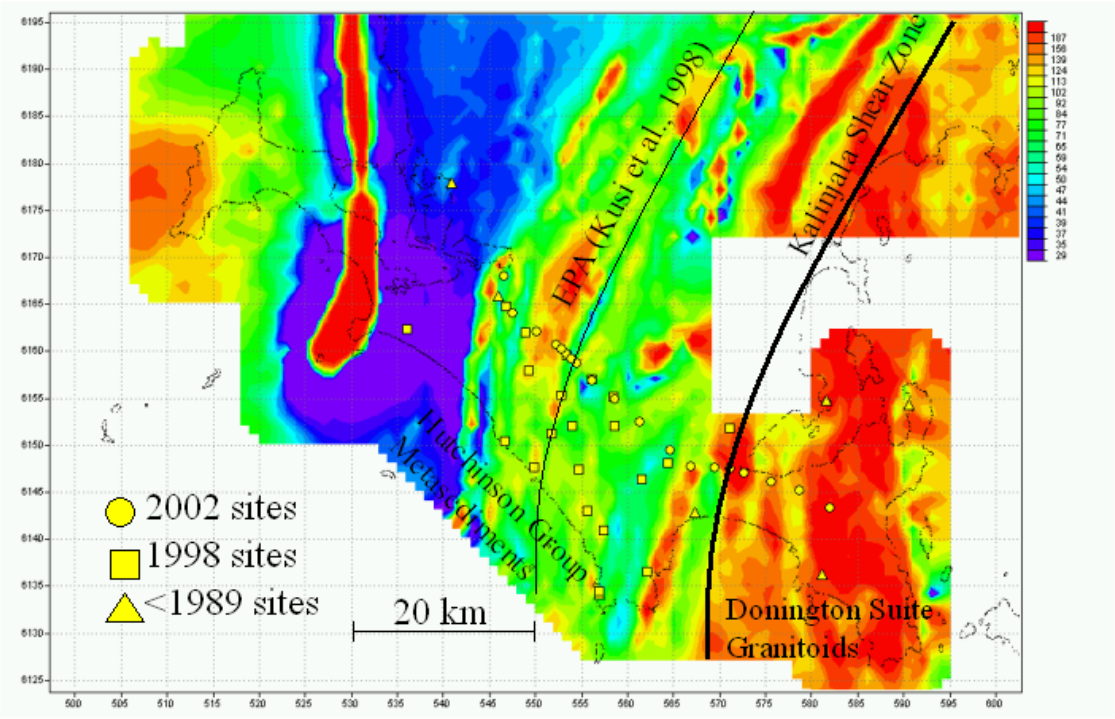

Figure 1: Map of southern Eyre Peninsula with sites from Milligan *et al.* (1989), Popkov *et al.* (2000) and SEACOAST experiment. Sites are plotted on top of Magnetic Anomaly image.

Sleaford metamorphic complex. To the east and west of the EPA, the surface layer is comprised of Hutchinson group metasediments (2.00-1.85 Ga) increasing in thickness towards the east. Further east there are exposures of the 1.85 Ga Donington Granitoid Suite, which is composed of granite intrusives, and basement reworked by the Kimban Orogeny (1.74-1.70 Ga). This event also led to intense deformation of the Hutchinson group metasediments (Vassallo & Wilson, 2002). The Kalinjala shear zone, as shown in Figure 1, separates the Donington Granitoid Suite from the Hutchinson group metasediments (Vassallo & Wilson, 2002).

Previous published surveys have dealt primarily with spatial mapping of resistivity anomalies, and have not had sufficient inter-site resolution and frequency bandwidth to model vertical geological structures in detail. This paper reports on forty new observation sites made in Southern Eyre Peninsula in 1998 (21 sites) and 2002 (19 sites). The more recent data set involved a newly developed three-component magnetometer system with faster sampling and larger dynamic range.

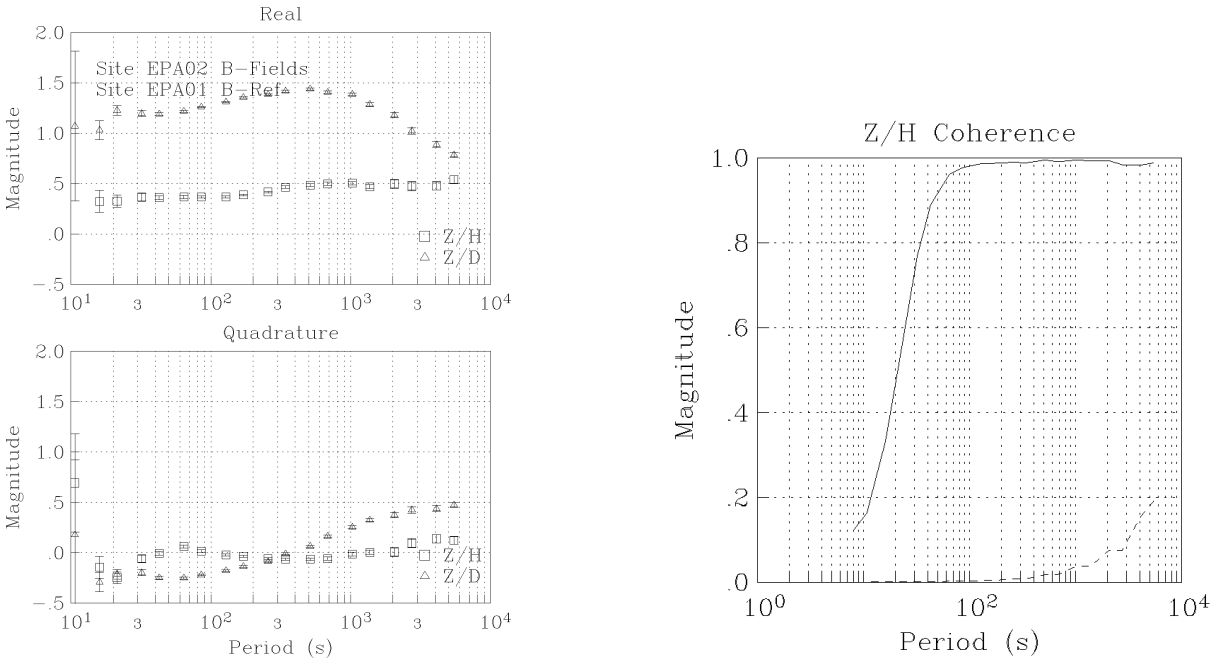

Figure 2: Coherences and transfer functions (real & quadrature) for site E02. Large real transfer functions indicate strong lateral resistivity contrast.

2 Field experiment

Nineteen sites were occupied along the disused BHP mineral sands railway line into the Lincoln National Park in southern Eyre Peninsula in July-August 2002. Four Magnetotelluric instruments developed at Flinders and Adelaide Universities recorded three-component magnetic fields at 20 Hz using a fluxgate magnetometer, with a precision of 10 pT and resolution of about 50 pT. The length of deployment ranged between a few hours and two days. At least two instruments recorded simultaneously in order to utilise one set of magnetic field data as remote-reference for the other set (Gamble *et al.*, 1979). In addition, twenty-one sites of magnetic observations recorded in 1998 during the SWAGGIE experiment were also included in the analyses (Popkov *et al.*, 2000).
Closer spacing of 1 km or less was chosen at locations across the Kalinjala Shear Zone (Vassallo & Wilson, 2002) and the previously identified strike of the EPA (Kusi *et al.*, 1998). This site-selection ensures a better resolution of variations in resistivity below the surface.

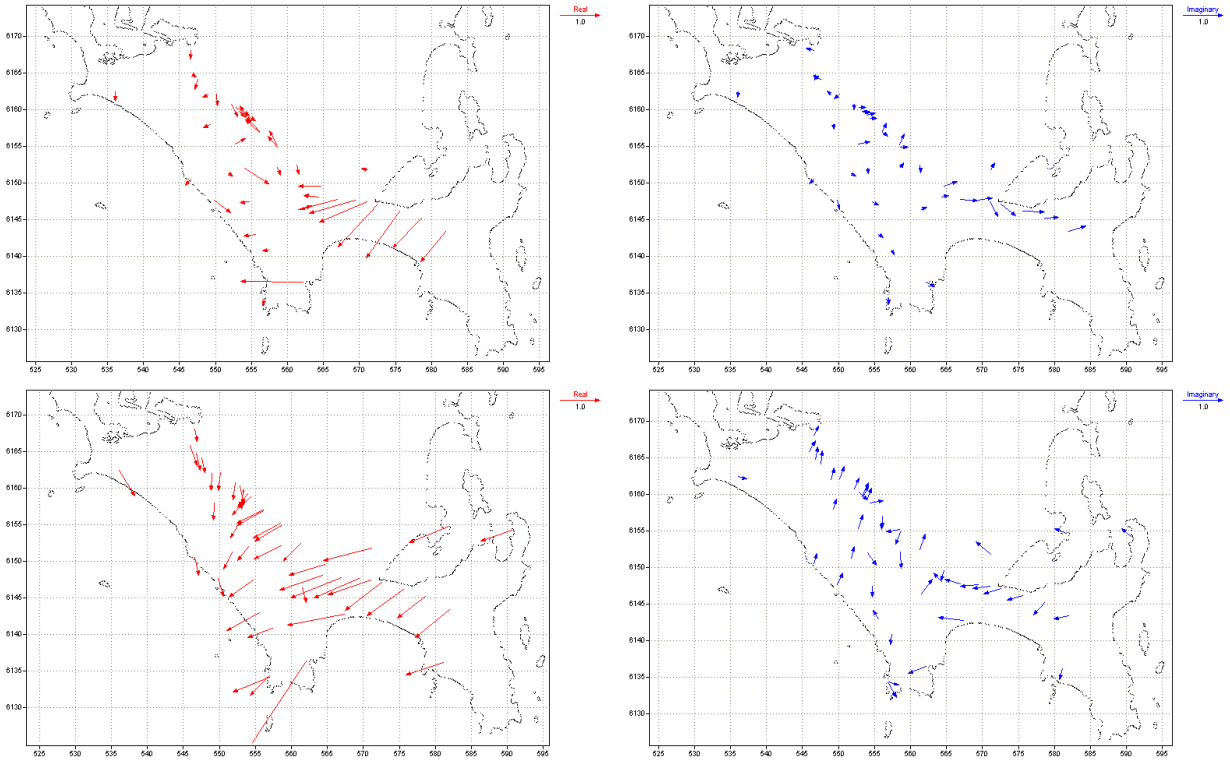

Figure 3: Parkinson GDS arrows for periods of 40 s and 2000 s. Red (blue) indicate real (quadrature) arrows.

3 Transfer functions and GDS arrows

The recorded time series are Fourier Transformed into the frequency domain using the robust remote-reference magnetotelluric (RRRMT) code of Chave & Thomson (1989). The response functions and the predicted coherences were then computed, using both conventional and robust remote reference methods (Figure 2). It shows that D (east-west) correlates more with Z (vertical downwards) than H (north-south) with Z, whereas

$$Z = \mathcal{A}H + \mathcal{B}D. \tag{1}$$

$\mathcal{A}$ and $\mathcal{B}$ denote the complex transfer functions. GDS arrows represent a linear relationship between components of the variation fields and are a graphical representation of the transfer functions $\mathcal{A}$ and $\mathcal{B}$ projected onto a plain (Parkinson, 1962). Lengths of the real M_r and quadrature M_q arrows are given by

$$M_r = \left([\Re(\mathcal{A})]^2 + [\Re(\mathcal{B})]^2 \right)^{1/2} \qquad M_q = \left([\Im(\mathcal{A})]^2 + [\Im(\mathcal{B})]^2 \right)^{1/2} \tag{2}$$

20. Kolloquium Elektromagnetische Tiefenforschung, Königstein, 29.09.-3.10.2003, Hrsg.: A. Hördt und J. B. Stoll

Orientation of the arrows is similarly determined by

$$\Phi_r = \tan^{-1}\left(\frac{[\Re(\mathcal{A})]^2}{[\Re(\mathcal{B})]^2}\right) \qquad \Phi_q = \tan^{-1}\left(\frac{[\Im(\mathcal{A})]^2}{[\Im(\mathcal{B})]^2}\right) \tag{3}$$

Orientations are clockwise positive from the x-direction (usually geomagnetic north). When plotted on a map Parkinson GDS arrows should "point" toward regions of high conductance and away from resistive blocks; to achieve this we follow the convention of Lilley & Arora (1982) and add 180° to each angle Φ_r and Φ_q to effectively reverse both real and quadrature arrows.

Figure 3 shows the real and quadrature GDS arrows obtained at all sites for periods of 40 s and 2000 s. Real GDS arrows always point directly towards the zone of highest conductance and away from resistive blocks. Shorter periods show comparatively small arrows on top of the Hutchinson group suggesting relatively low resistivity contrast around the sites (approximately 5-15 km). By comparison, sites on the Donington Granitoid Suite have large GDS arrows. Since the underlying crystalline rock has higher resistivity, the sites are sensitive to resistivity structures further away, including the conductive seawater.

4 Geophysical Modelling

Real and quadrature parts of the GDS arrows were inverted for 2D resistivity structure using the non-linear conjugate gradient (NLCG) algorithm of Rodi & Mackie (2001), and the Occam inversion algorithm. Two profiles were chosen that cross the major tectonic boundaries orthogonally with 6 and 19 stations, respectively. Magnetic field transfer functions $\mathcal{A}$ and $\mathcal{B}$ were projected along the profile orientations assuming that the structure is predominantly 2D. Inversions were then carried out using these projected transfer functions for twenty periods spaced uniformly in logarithmic intervals between 8 and 5461 s. Starting model for both profiles was a half-space of 100 Ωm to a depth of 125 km. Topography information, collected with GPS instruments during the experiment, was included in the inversion process.

Resistivity structure

The NLCG model for the 19 sites-profile is illustrated in Figure 4 as representative for all obtained models, which show similar structure for both different inversion algorithms and profiles. All models show a arcuate-shaped, very low resistivity ($< 1\ \Omega$m) structure close to the surface and up to 5 km deep (labelled A in Figure 4). This conductive feature

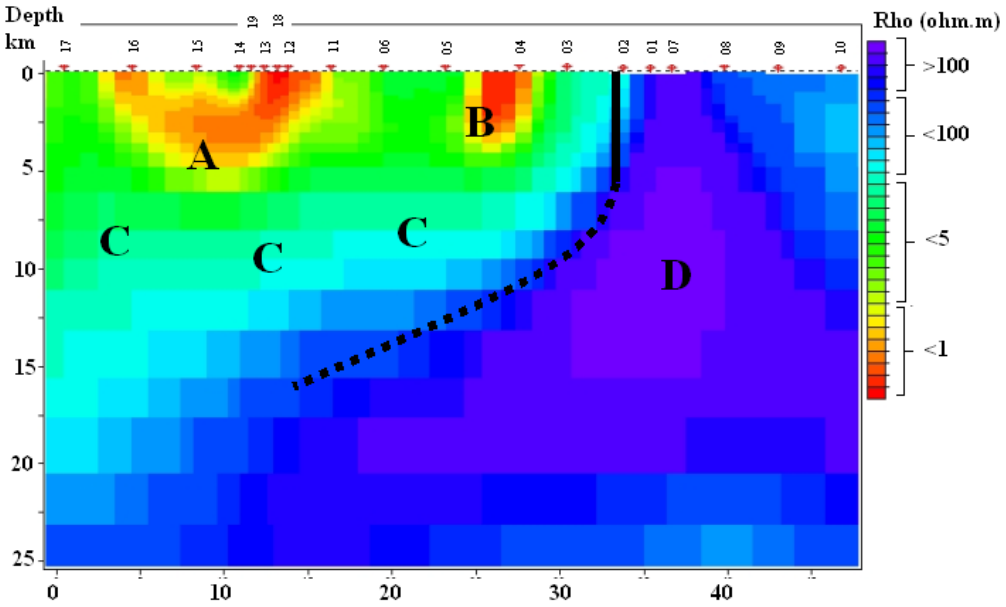

Figure 4: NLCG-Inversion results for profile, othogonal to strike of major tectonic boundaries, with 19 stations deployed in 2002.

has been identified as the Eyre Peninsula Anomaly (EPA) (White & Milligan, 1984). A second prominent shallow feature occurs beneath sites 4 close to the Uley graphite mine and is labelled B. Sleaford complex, labelled C, shows a low resistivity of between 10 to 100 Ωm, increasing in depth to the west and reaching up to 20 km beneath site 17. Adjacent to the conductive Archaean Sleaford Complex is the resistive ($>$ 100 Ωm) Donington Granitoid Suite, labelled D, with a steeply-dipping interface. It should be noted that GDS measurements provide only approximate depth determination of the base of conductors, but similar values from both inversions give confidence in the depth estimates. The total conductance beneath site 14, representing the centre of the EPA, is around 10000 S, similar to the estimate of Kusi *et al.* (1998).

A Bouguer gravity forward model has been developed representing all structures labelled A to D in Figure 4 as well as younger Quarternary sediments on top of the Sleaford complex. Density values follow sample values taken in the field. The included structures of the gravity model were constrained from the resistivity model in Figure 4 reinforcing the idea of the extensional regime between 2.00-1.85 Ga and before the Kimban Orogeny. Figure 1 shows that zones of high magnetic susceptibility correlate well with low resistivities in the Hutchison Group (regions A and B in Figure 4).

20. Kolloquium Elektromagnetische Tiefenforschung, Königstein, 29.09.-3.10.2003, Hrsg.: A. Hördt und J. B. Stoll

5 Geophysical Interpretation

The 2D models reveal a complex structure, which has not been reported by previous studies (White & Milligan, 1984; Kusi *et al.*, 1998). Clearly visible in Figure 4 is the steeply-dipping resistivity contrast between zones C and D, which coincides with the location of the Kalinjala Shear Zone on the surface. It is suggested that the resistivity boundary represents a growth fault that is typical for rift systems that evolve into a half-graben structure due to extensional forces (Price & Faulds, 1997).
The very low resistivity zone B in Figure 4 is presumably graphite, which has been mined at Uley. A likely cause for the EPA low resistivity zone A is also graphite. Saline fluids in upper-crustal (top 8 km) fractures are not stable enough over long time intervals, and it is difficult to obtain observed low resistivity unless fluids are extremely saline or unrealistically hot. Sulphide occurrences have been evoked as a possible mechanism for similar anomalies in North America, but have not been reported from drilling in this area.

The source of graphite is most probably thermal metamorphism of carbonaceous sediments. This reaction commonly occurs at mid-crustal depths over long time periods, where temperatures are 250-450 °C. Subsequent shearing of the metasediments, with redistribution and smearing out of the graphite, then has the potential to create upper-crustal resistivity anomalies.
It can be seen that the upper crustal zones A and B of very low resistivity correlate with the highly-magnetic banded iron formations. A shallow marine environment has to be present to produce banded iron formation deposits, and Lemon (1980) suggested a north-south trending shoreline between 2.00-1.85 Ga. Chemical reactions abundant in the presence of Cyanobacteria produced Ferric ions, the main components in the iron-rich layers of banded iron formations. Biogenic material decomposed into methane (CH_4) and carbon dioxide (CO_2) providing the reactants to yield carbon.

The arcuate shape of region A suggests a compressive origin possibly during the Kimban Orogeny, which led to folding of Hutchinson Group metasediments and enrichment of graphite in the hinges. Carbon zones may also preferentially accommodate shearing due to lower shear strength, and thus can be found along faults such as occurs at Uley.
It is more difficult to explain the origin of relatively low resistivities of $10 - 100\,\Omega$m in the Sleaford Complex (region C). It is suggested that either secondary porosity in small-scale fractures, or an additional grain-boundary conducting mechanism may reduce the

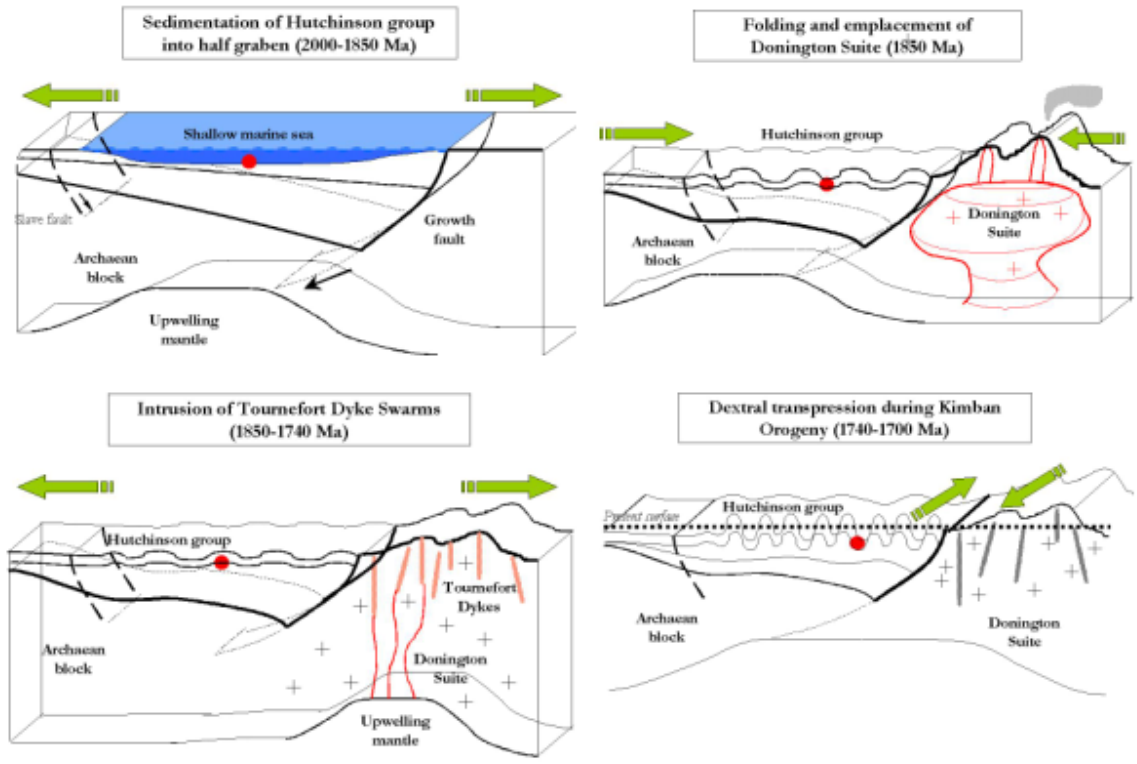

Figure 5: Conceptual tectonic model of southern Gawler Craton between 2.00-1.7 Ga.

resistivity compared with the Donington granitoids. However a certain smoothing effect in the inversion process between the highly conductive regions A and B and the resistive Donington Granitoid Suite labelled D should not be underestimated.

6 Discussion and Conclusion

Figure 5 shows a conceptual interpretation of processes that might have led to the tectonic and resistivity structures imaged in Figure 4. Hutchinson Group sediments were deposited between 2.00-1.70 Ga. On the basis of U-Pb zircon dates of inherited zircons, it was suggested that basin formation occurred via gradual lithospheric extension accommodating a series of mixed chemical and clastic sediments within a shallow marine basin increasing in thickness towards the east. Lemon (1980) also suggested that the Hutchinson Group was deposited in a shallow sea with a north-south trending shoreline. The occurrence of banded iron formations trending north-south supports this hypothesis. Hutchinson metasediments includes the Warrow Quartzite and the Cook Gap Schists,

20. Kolloquium Elektromagnetische Tiefenforschung, Königstein, 29.09.-3.10.2003, Hrsg.: A. Hördt und J. B. Stoll

the latter of which is equated with the Uley graphite.
Around 1.85 Ga ago, a compressional event resulted in folding of the Hutchinson Group. To the east granitoids were emplaced forming the Donington Granitoid Suite (Vassallo & Wilson, 2002). The westward dipping character and the narrow width of the Kalinjala Shear Zone rule out this structure as a subduction zone related to the emplacement of these granitoids.

Between 1.85-1.74 Ga an extensional event followed producing regional-scale mafic dyke swarms (Tournefort dykes) striking north-south, and magmatically involved sub-basins that probably developed in a continental interior setting. After this extension event, the Kimban Orogeny reworked most of the Hutchinson Group material during the interval (∼1.74-1.70 Ga) (Vassallo & Wilson, 2002). Folding resulted in anticline and syncline structures within the Hutchinson Group metasediments. The Kimban Orogeny was characterised by dextral transpression, resulting in the development of the Kalinjala Shear Zone (Vassallo & Wilson, 2002).

7 Acknowledgements

The authors thank the Australian Society Exploration Geophysicists, Primary Industries and Resources, South Australia (PIRSA), Flinders University and Adelaide University and a Deutscher Akademischer Austauschdienst (DAAD) scholarship for financial support in this experiment. Mr Michael Schwarz (PIRSA), Dr. P.R. Milligan and Dr. L.J. Wang of Geoscience Australia provided geophysical data.

References

Chave, A.D., Thomson, D.J., 1989. Some comments on magnetotelluric response function estimation. *J.Geophys.Res.*, 94, 14215-14225.

Gamble, T.D., Goubau, W.M., Clarke, J., 1979. Magnetotellurics with a remote magnetic reference. *Geophysics*, 4, 53-68.

Kusi, R., White, A., Heinson, G., Milligan, P., 1998. Electromagnetic induction studies in the Eyre Peninsula, South Australia. *Geophys. J. Int.*, 132, 687-700.

Lemon, N.M., 1980. The Middleback Subgroup. In: Symposium on the Gawler Craton. *Journal of the Geological Society of Australia*, 27, 45-53.

Lilley, F.E.M., Arora, B.R., 1982. The sign convention for quadrature Parkinson arrows in geomagnetic induction studies. R*eviews of Geophysics and Space Physics*, 20, 513-518.

Milligan, P.R., White, A., Chamalaun, F.H., 1989. Extension of the Eyre Peninsula conductivity anomaly. *Exploration Geophys.*, 20, 187-190.

Parkinson, W.D., 1962. The influence of continents and oceans on geomagnetic variations. *Geophys. J. R. Astron. Soc.*, 6, 441-449.

Popkov, I., White, A., Heinson, G., Constable, S., Milligan, P., Lilley, F.E.M., 2000. Electromagnetic investigation of the Eyre Peninsula conductivity anomaly. *Exploration Geophysics*, 31, 187-191.

Price, L.M., Faulds, J.E., 1997. Geometry and evolution of a major segment of the Grand Wash fault zone, southern White Hills, northwestern Arizona. In: *Geological Society of America*, 1997 annual meeting. Anonymous Abstracts with Programs - Geological Society of America, 29; 6, 375-376.

Rodi, W., Mackie, R.L., 2001. Nonlinear conjugate gradients algorithm for 2-D magnetotelluric inversion. *Geophysics*, 66, 174-187.

Vassallo, J.J., Wilson, C.J.L., 2002. Palaeoproterozoic regional-scale non-coaxial deformation: an example from eastern Eyre Peninsula, South Australia. *Journal of Structural Geology*, 24, 1-24.

White, A., Milligan, P.R., 1984. A crustal conductor on Eyre Peninsula, South Australia. *Nature*, 310, 219-222.